Fuel-optimal look-ahead adaptive cruise control for heavy-duty vehicles

Valerio Turri*, Oscar Flärdh♯, Jonas Mårtensson*‡, and Karl H. Johansson*

***Abstract*— In this paper, we investigate the problem of how to optimally control a heavy-duty vehicle following another one, commonly referred as "ad-hoc" or "non-cooperative platooning". The problem is formulated as an optimal control problem that exploits road topography information and the knowledge of the preceding vehicle speed trajectory to compute the optimal engine torque and gear request for the vehicle under control. The optimal control problem is implemented by dynamic programming and is tested in a simulation study that compares the performance of multiple longitudinal control strategies. The proposed look-ahead adaptive cruise controller is able to achieve fuel saving up to 7 % with respect to the use of a reference controller, by combining the benefits of adjusting the inter-vehicular distance according to the future slope with those of alternating phases of throttling and coasting.**

I. INTRODUCTION

Throughout the last two decades developed countries have put enormous efforts in reducing man-related greenhouse gas emissions and energy consumption [1], [2]. While in almost all sectors those efforts were successful, greenhouse gas emissions related to road freight transportation are still increasing [3], [4]. This is mainly imputable to the unmatched flexibility of using heavy-duty vehicles for freight transport and to the continuously increasing request for transported goods. Because of the strong link between economical growth and amount of transported goods [5], inverting this trend is extremely difficult.

In this paper, we study how vehicle-following control strategies can be exploited to reduce the fuel consumption and, consequently, the greenhouse gas emissions of heavy-duty vehicles. In particular, we investigate how the benefits of short inter-vehicular distance and freewheeling can be combined to maximize the fuel savings.

Thanks to the fuel reduction potential, the adoption of these control strategies is not only beneficial for the environment but also for transportation businesses. The impact of the fuel cost for a single long-haulage truck is estimated to account for more than one third [6] of the total cost for operating a long-haulage truck. When long-haulage truck will be autonomous, this percentage is expected to raise significantly thanks to the absence of the truck driver in the cabin and the possibility to continuously drive the truck. In order to maintain competitiveness, we believe that the adoption of these control strategies will be therefore crucial for the autonomous transportation companies of the future. A 15 % fuel consumption reduction (achievable with these control strategies as shown in Section VI) for an autonomous truck driving 20 hours a day for 350 days a year translates into approximately 30 thousand euros saved each year per truck[1].

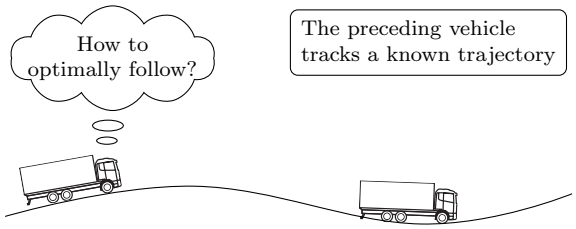

Fig. 1. Sketch of the problem under study.

Vehicle platooning is a well-known control problem with research papers on the topic appearing since the sixties. The majority of these works studied platooning as a mean for increasing traffic density [7], reducing road accidents [8], [9] and facilitating the deployment of autonomous vehicles [10] (refer to [11] for a full survey). Those works, therefore, focused on solving problems related to string stability [12], [13], platoon safety [9] and wireless network control [14] (refer to [11] for a full survey). Only in the recent years the fuel saving potential of platooning gained the interest of the research community and industry. Thanks to the particular shape of heavy-duty vehicles, the short inter-vehicular distance achievable with platooning control creates a slipstream effect that results in the reduction of the fuel consumption. Tests conducted in controlled environment and flat road showed that by using simple PI controllers to track a defined gap policy, follower heavy-duty vehicles can save up to 10 % of fuel [15], [16]. However, the varying topography of real roads requires the use of more sophisticated controllers (referred as "look-ahead") that rely on the optimal control framework to embed road topography information. In the literature, the optimization problem returned by the optimal control problem has been solved both using quadratic programming [17] and dynamic programming [18]. These approaches, however, are not suitable to explore the benefits of freewheeling strategies while driving in a platoon formation.

* ACCESS Linnaeus Centre and the Department of Automatic Control, KTH Royal Institute of Technology, Stockholm, Sweden, email: turri, jonas1, kallej@kth.se.

♯ Scania CV AB, SE-15187 Södertälje, Sweden, email: oscar.flardh@scania.com.

‡ Integrated Transport Research Lab(ITRL), KTH Royal Institute of Technology, Stockholm, Sweden.

[1]The calculation assumes a truck average speed of 80 km/h, a fuel efficiency of 0.3 l/km and a fuel cost of 1.30 €/l.

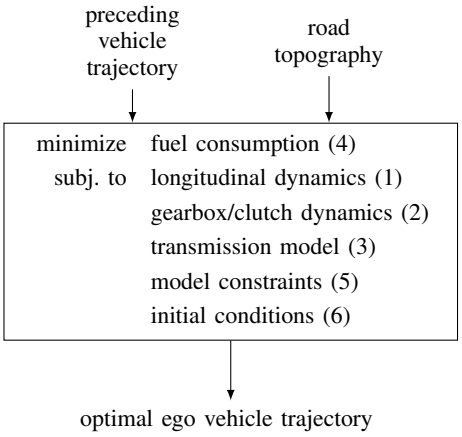

Fig. 2. Formulation of the optimal control problem.

In this work, we study the control problem of how to fuel-optimally follow a vehicle whose future trajectory is assumed to be known, as sketched in Figure 1. The contributions of this paper are threefold. First, the optimal control problem is formulated in such a way that both the benefits from keeping a short inter-vehicular distance and from the use of freewheeling can be explored. Second, the implementation of the optimal control problem through dynamic programming is discussed. Finally, a comparison of the performance of multiple longitudinal control strategies achievable with the proposed controller is presented. The simulation study shows how it is possible to combine the benefits of short inter-vehicular distance with those of freewheeling, reaching fuel saving of up to 18 % by keeping a minimum distance of 20 m.

The remainder of the paper is organized as follows. Section II introduces the optimal control problem formulation, while Sections III and IV characterize it by presenting the vehicle model, the fuel model and the model constraints. Section V discusses the dynamic programming implementation. Section VI presents the simulation study. Finally, Section VII concludes the paper suggesting possible future research directions.

II. OPTIMAL CONTROL PROBLEM

The problem of minimizing the vehicle fuel consumption is formulated as the optimal control problem sketched in Figure 2. Topography information is assumed to be available and, if a preceding vehicle exists, its future speed trajectory is assumed to be known by the vehicle under control. This can be achieved by communication or by estimation. Such scenario can be interpreted as a non-cooperative or ad-hoc platoon, where the following vehicle computes the optimal input given the knowledge of the trajectory of the preceding vehicle.

Remark *It is not in the scope of the paper to take updates of the preceding vehicle speed trajectory into account. Even if changes in the preceding vehicle trajectory can be easily exploited using a receding horizon framework, the optimality of bang-bang control trajectories can lead to sharp increases of the cost function when the preceding vehicle trajectory is updated. This can happen, for example, during a downhill, if the vehicle under control follows a costing trajectory that leads to the minimum allowed distance at the end of the downhill. If the preceding vehicle speed trajectory is updated with a slower one, the feasibility of the problem requires the vehicle under control to brake, resulting therefore in a inefficient behavior. A discussion on how this problem can be overcome when a receding horizon approach is used is presented in Section VII. In this work, we assume that the preceding vehicle exactly follows the communicated speed trajectory.*

The vehicle under control is modeled as a hybrid system. Its continuous states are the vehicle speed v and the distance to the preceding vehicle d (collected in the vector $x = [v,\, d]^{\mathrm{T}}$), while its discrete state is the current gearbox/clutch state g. Its continuous control input are the engine torque T and braking force F_b (collected in the vector $u = [T,\, F_b]^{\mathrm{T}}$), while its discrete control input is the gearbox request g_r. The vehicle model includes:

- the non-linear longitudinal dynamics
$$\dot{x} = f_1(x, F_e, F_b), \tag{1}$$
where F_e is the longitudinal force generated by the powertrain;
- the gearbox/clutch dynamics modeled by the timed automaton
$$(g^+, \tau^+) = f_2(g, g_r, \tau), \tag{2}$$
where τ is the automaton clock;
- the transmission model defining the static relation between the engine variables (engine torque T and speed ω) and the chassis variables (longitudinal powertrain force F_e and vehicle speed v), i.e.,
$$F_e = F_e(g, T), \quad \omega = \omega(v, g). \tag{3}$$
In order to limit the model complexity, the engine inertia is approximated to zero. This allows to ignore the engine dynamics and to define the engine speed as a state-dependent variable rather than a state, resulting in a significantly reduced complexity of the dynamic programming implementation.

The expressions of the vehicle model functions $f_1(\cdot,\cdot,\cdot)$, $f_2(\cdot,\cdot,\cdot)$, $F_e(\cdot,\cdot)$ and $\omega(\cdot,\cdot)$ are discussed in Section III.

The objective of the optimal control problem is to minimize the vehicle fuel consumption over the time horizon H,
$$\int_{t_0}^{t_0+H} q(T, \omega) dt, \tag{4}$$
where $q(\cdot,\cdot)$ is the static map describing the fuel flow as a function of the engine operation point and t_0 is the optimization initial time. The vehicle is subjected to input and state constraints summarized by
$$c(x, u, g, g_r) \in \mathcal{C}. \tag{5}$$

TABLE I
MODEL PARAMETERS

g_a	gravitational acceleration	m/s^2	9.81
c_r	rolling coefficient	-	0.005
$C_{d,0}$	nominal drag coefficient	-	0.6
$C_{d,1}$	first drag reduction coefficient	m^{-1}	12.8
$C_{d,2}$	second drag reduction coefficient	m	19.7
τ_{fw}	freewheel minimum time	s	8
τ_{shift}	gear-shift time	s	1
ω_{min}	minimum engine speed	rpm	500
ω_{max}	maximum engine speed	rpm	2000

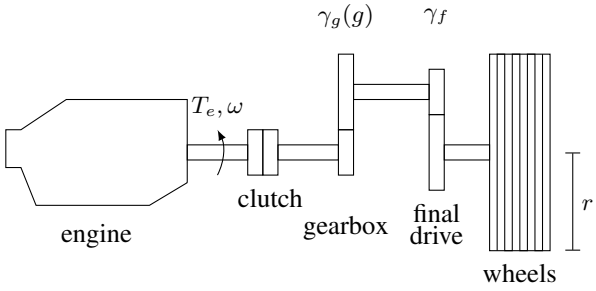

Fig. 3. Illustration of the powertrain.

These constraints include speed limits, bounds on the distance range, on the engine speed/torque and on the braking force. The full characterization of these constraints and the expression of $q(\cdot,\cdot)$ is given in Section IV.

By adding initial conditions on the states

$$\begin{aligned} x(t_0) &= x_0, \\ g(t_0) &= g_0, \end{aligned} \tag{6}$$

the optimal control problem can be summarized by the formulation in Figure 2.

The optimal control problem is implemented using dynamic programming. This is motivated by the discrete dynamics of the gearbox and the non-linearities in the longitudinal dynamics and fuel consumption models that make the overall optimization problem extremely nonlinear. The dynamic programming implementation is discussed in Section V.

III. VEHICLE MODEL

In this section we present the vehicle model used in the optimal control problem formulation. The vehicle model is composed of the longitudinal dynamics and the powertrain model. The powertrain model is split, in its turn, into the gearbox/clutch dynamics model and the static transmission model.

A. Longitudinal dynamics

The longitudinal vehicle dynamics introduced in (1) are described by the differential equations

$$\dot{x} = \begin{bmatrix} \dot{v} \\ \dot{d} \end{bmatrix} = f_1(x, F_e, F_b) = \begin{bmatrix} \frac{1}{m}\left(F_e + F_b + F_{\text{ext}}(x)\right) \\ v_{\text{f}} - v \end{bmatrix}. \tag{7}$$

The first equation represents the force balance with respect to the longitudinal direction, where the term

$$F_{\text{ext}}(x) = -mg\sin\alpha(s_f - d) - mg_a c_r - \frac{1}{2}\rho C_d(d) v^2$$

collects all the external forces acting on the vehicle, i.e., the gravitational, the rolling and the aerodynamic forces, respectively. The second equation defines the distance dynamics. The time-variant parameters v_f and s_f represent the longitudinal position and speed of the rear end of the preceding vehicle, respectively. The state-dependent parameter $\alpha(s)$ denotes the road slope at longitudinal position s. These parameters are assumed to be known. The definition of the remaining static parameters, and their values, are provided in Table I.

The aerodynamic coefficient C_d is expressed as a non-linear function of the distance to the preceding vehicle d according to

$$C_d(d) = C_{d,0}\left(1 - \frac{C_{d,1}}{d + C_{d,2}}\right), \tag{8}$$

where $C_{d,0}$, $C_{d,1}$ and $C_{d,2}$ are static parameters whose value is displayed in Table I (see [18] for a more detailed discussion).

Remark *If the vehicle under control is driving alone (i.e there is no preceding vehicle), the longitudinal dynamics model* (7) *can be still used with minor changes. In particular, the state* d *is redefined as the distance to a virtual vehicle driving at a constant speed and* $C_d(d)$ *as the constant value* $C_{d,0}$.

B. Gearbox/clutch dynamics

An illustration of the whole powertrain is displayed in Figure 3. In this section, we focus on modeling the discrete dynamics characterizing the gearbox and the clutch. This model, combined with the correct characterization of the transmission (presented in the next subsection), allows to capture the absence of transmitted power during gear shifts and freewheeling.

The gearbox/clutch dynamics is modeled by the timed automaton displayed in Figure 4 and previously introduced by equation (2). The state of the automaton is $g \in \{-1,\, 0\} \cup \mathcal{G}$, where $\mathcal{G} = \{i \in \mathbb{N} | i \in [g_{\text{min}},\, g_{\text{max}}]\}$ represents the set of the admissible gears. If $g \in \mathcal{G}$, the clutch disks are closed and gear g is engaged. If $g = 0$, the clutch disks are open and the vehicle is freewheeling. Finally, if $g = -1$, the clutch disks are open and a gear shift is taking place. The control input of the automaton is $g_r \in \{0\} \cup \mathcal{G}$. If $g_r \in \mathcal{G}$, gear g_r is requested, while, if $g_r = 0$, freewheeling is requested. The time requirements on the gear shifts and the freewheeling are ensured by edge guards and location invariants.

The gearbox starts in the engaged gear condition, i.e., $g_0 \in \mathcal{G}$. This is modeled by the central macro-state in the automaton of Figure 4 that collects all the state $g \in \mathcal{G}$. From this macro-state, two transitions are possible:

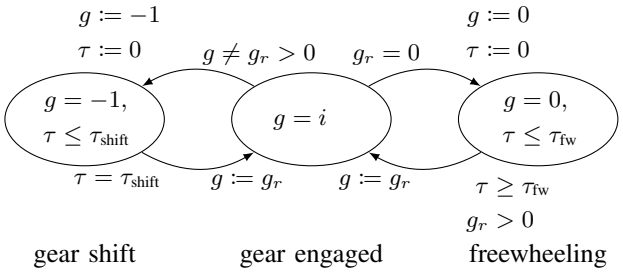

Fig. 4. Model of the gearbox/clutch dynamics.

- if the requested gear g_r switches to 0, the gearbox jumps to the freewheeling state, i.e., $g = 0$. In order to avoid a premature deterioration of powertrain components and driver discomfort, the fast switching between engaged gear and freewheeling is limited by requiring that the freewheeling is maintained for a time longer than τ_{fw}. This is achieved by resetting the automaton clock τ, when the gearbox jumps to $g = 0$, and by defining the location invariant $\tau \leq \tau_{\text{fw}}$ for the freewheeling state and the guard $\tau \geq \tau_{\text{fw}}$ on the edge leaving the freewheeling state. If we are not interested in exploiting freewheeling, the requested gear set can be redefined as $g_r \in \mathcal{G}$.
- if the requested gear g_r switches to a value in the set $\mathcal{G}$ different from g, the gearbox jumps to the gear-shift state, $g = -1$. The gearbox stays in the gear-shift state for a time of τ_{shift}, before jumping to the engaged gear macro-state with $g = g_r$.

C. Transmission model

Here, we discuss the static transmission model introduced in equation (3) that defines the relation between the engine variables and the chassis variables as function of the gearbox/clutch state g. This model completes the powertrain model sketched in Figure 4.

The torque T generated by the engine acts on the engine side of the clutch. If the clutch disks are open (i.e, $g \in \{-1, 0\}$, no torque is transmitted by the gearbox/clutch group. If a gear is engaged (i.e, $g \in \mathcal{G}$), the torque is amplified by a factor $\gamma_g(g)$ depending on the specific engaged gear g. In order to account for the transmission losses, an efficiency gear-dependent term $\eta(g)$ is included in the torque model transmission. The torque on the gearbox shaft is transmitted to the wheel shaft by the final drive that amplifies it by a constant factor γ_f. Finally, the torque on the wheel shaft is transfered on the road by the wheels. The longitudinal force F_e generated by the road/wheel contact can be therefore summarized by

$$F_e(g, T) = \begin{cases} 0, & \text{if } g \in \{-1,\, 0\}, \\ \frac{\eta(g)\gamma_g(g)\gamma_f}{r} T, & \text{if } g \in \mathcal{G}, \end{cases} \tag{9}$$

where r is the wheel radius.

In a similar way we can compute the relation between the vehicle speed and the engine speed, obtaining

$$\omega(g, v) = \begin{cases} \omega_{\text{min}}, & \text{if } g \in \{-1,\, 0\}, \\ \frac{\gamma_g(g)\gamma_f}{r} v, & \text{if } g \in \mathcal{G}. \end{cases} \tag{10}$$

Note that, when the clutch is open, the engine is assumed to rotate at the minimum allowed engine speed ω_{min}.

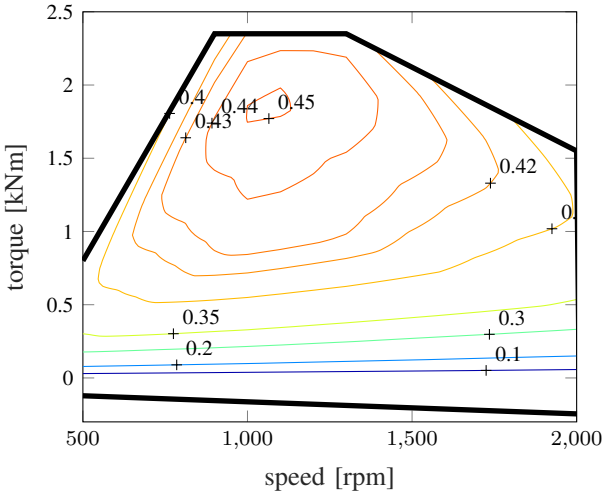

Fig. 5. Realistic BSFC map of a 450 hp engine used in the simulation. The map has been obtained by modifying the original map of a real Scania engine.

IV. FUEL MODEL AND VEHICLE CONSTRAINTS

In this section, we present the fuel consumption model and the vehicle constraints.

A. Fuel model

The vehicle fuel consumption is computed by integrating the fuel flow over time as introduced in (4). In this work, the fuel flow is modeled as a static map of the engine torque T and engine speed ω, i.e., $q(T, \omega)$. This map is related to the more-known brake specific fuel consumption (BSFC) map that defines the engine efficiency (generated engine power per consumed fuel) as a function of the engine torque and speed. The BSFC map can be obtained by gridding the torque/speed space and measuring the engine fuel consumption and the generated power for each grid point. Figure 5 displays the BSFC map of the engine used in the simulation. This map represents a 450 hp engine that has been obtained by modifying the original map of a real Scania engine.

B. Vehicle constraints

In this section, we present the constraints acting on the vehicle model summarized by (5):

- the engine speed and torque are bounded by

$$\begin{aligned} \omega_{\text{min}} \leq \omega \leq \omega_{\text{max}}, \\ T_{\text{min}}(\omega) \leq T \leq T_{\text{max}}(\omega). \end{aligned} \tag{11}$$

The limitations on the engine speed and the upper bound on the torque are necessary to guarantee the

correct functioning of the engine. The lower bound on the torque, instead, represents the braking engine torque when no fuel is injected. These limits have been depicted in Figure 5 as black lines;

- the vehicle speed is bounded by

$$v_{\text{min}} \leq v \leq v_{\text{max}} \tag{12}$$

in order to take speed limits into account. For the sake of simplicity, the speed limits are assumed to be constant, although space-varying speed limits can be handled with no increase of the problem complexity;

- the distance is bounded by

$$d_{\text{min}} \leq d \leq d_{\text{max}}. \tag{13}$$

In the case of the vehicle-following scenario, the lower and upper bounds represent the safe and maximum distance allowed for platooning, respectively. In the case of the vehicle driving-alone, the bounds on the distance can be chosen large enough such that the resulting optimal trajectory do not reach them. Note that bounds on the distance are necessary for solving the optimal control problem with dynamic programming.

- the braking force is bounded by

$$F_{\text{b,min}} \leq F_{\text{b}} \leq 0. \tag{14}$$

V. DYNAMIC PROGRAMMING IMPLEMENTATION

In this section, we first discuss how the optimal control problem summarized in Figure 2 is implemented using dynamic programming and, second, we analyze the complexity of such implementation as function of the dynamic programming parameters.

A. Bellman equation

In order to use the dynamic programming framework, discretization over time, and over the continuous input and states, is carried out. We denote with n_v, n_d, n_T and n_{F_b} the number of discretization points for the speed, the distance, the torque and the braking force, respectively. Δt denotes the discretization time, while $N = \lceil H/\Delta t \rceil$ the number of time steps over the prediction horizon[2]. The new discretized inputs and states are represented by adding the time step subscript i to the original variables, e.g., $x_i = x(i\Delta t)$. Such discretization allows to apply the Bellman equation [19] to the presented optimal control problem, obtaining the following expression:

$$\begin{aligned} J_i(x_i, g_i) = \min_{u_i, g_{r,i}} \Big\{ & \phi_j(x_i, g_i, u_i, g_{r,i}) \\ & + \tilde{J}_{i+j}(\psi_j(x_i, g_i, u_i, g_{r,i}), g_{r,i}) \Big\}, \end{aligned} \tag{15}$$

where

- $J_i(x_i, g_{r,i})$ represents the cost-to-go at time $i\Delta t$ (i.e., the optimal fuel consumption from $i\Delta t$ until the end of the horizon H) as function of the current state $[x_i, g_i]^{\text{T}}$;
- $\phi_j(x_i, g_i, u_i, g_{r,i})$ represents the local fuel cost from time $i\Delta t$ to time $(i+j)\Delta t$ by starting from state $[x_i, g_i]^{\text{T}}$ and applying input $[u_i, g_{r,i}]^{\text{T}}$. The fuel cost has been obtained by simulating the vehicle model (1–3) and integrating (4);
- $\psi_j(x_i, g_i, u_i, g_{r,i})$ represents the state x_{i+j} obtained by simulating the vehicle model (1–3) for time $j\Delta t$ with initial condition $[x_i, g_i]^{\text{T}}$ and input $[u_i, g_{r,i}]^{\text{T}}$;
- $\tilde{J}_i(\cdot, \cdot)$ extends the map $J_i(\cdot, \cdot)$ to the points between the discretized states by linear interpolation.

The aforementioned simulations between the dynamic programming time steps are carried out using the explicit Euler method with discretization time $\Delta t_{\text{sim}} \leq \Delta t$. By defining the final cost $J_N(\cdot, \cdot) = 0$ and proceeding backward, equation (15) can be exploited to compute a closed-loop control law for each time step $i \in \{0, .., N-1\}$.

Unlike the conventional Bellman equation, the number of local time steps j is not limited to 1, but is a function of the current state and input, i.e., $j = j(x_i, g_i, u_i, g_{r,i})$. This is exploited, for example, when we compute the argument of $\min\{\cdot\}$ in equation (15) for $g_i \in \mathcal{G}$ and $g_{r,i} = 0$ (i.e, the cost of requesting freewheeling when a gear is engaged), and $\tau_{\text{fw}} > \Delta t$. Since, after requesting freewheeling, no control input can affect the state for a time span of τ_{fw}, the vehicle model can be simulated for a time of $j\Delta t$, where $j = \lceil \tau_{\text{fw}}/\Delta t \rceil$. In this way, the clock τ of the automaton does not need to be treated as a state in the dynamic programming implementation resulting in a reduced complexity of the algorithm.

B. Complexity analysis

At each time step $i \in \{0, .., N-1\}$ and for each pair $(x_i, g_{r,i})$, we solve the Bellman equation (15). Solving each instance of the Bellman equation requires to compare as many cost values as the number of possible input combinations. We note however that the inputs T and F_b are intuitively mutually exclusive, i.e., it is inefficient to throttle and brake at the same time. The complexity $\mathcal{C}$ of the dynamic programming implementation is therefore

$$\mathcal{C} = \mathcal{O}(N n_v n_d (n_T + n_{F_b}) n_g), \tag{16}$$

where n_g denotes the number of gears including freewheeling, if exploited. If necessary for real-time implementation, the complexity can be further reduced, for example, by limiting the state space to the robust control invariant set.

VI. SIMULATION STUDY

In this section, we analyze the performance of the proposed controller by means of simulations. After introducing the simulation setup, we compare the performance of multiple longitudinal control strategies achieved with the proposed controller, including control strategies for the vehicle driving alone and following another one. The study is conducted considering different masses of the vehicle under control and same mass for the preceding one. This allows to analyze how the performance of the various control strategies is affected by the mass distribution in the platoon.

[2]The operator $\lceil \cdot \rceil$ denotes the upper integer approximation of the argument.

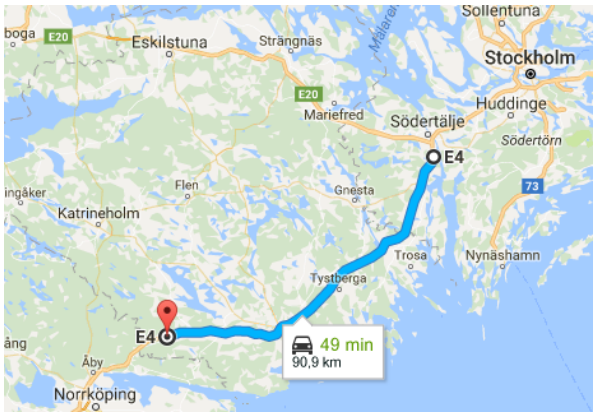

Fig. 6. Benchmark highway stretch between the cities of Södertalje and Jönåker, Sweden (Map data ®2017 Google).

TABLE II

CONTROLLER PARAMETERS

all control strategies			
H	prediction horizon	s	3800
Δt	DP discretization time	s	4
Δt_{sim}	DP integration time	s	1
$v_{\min}$	minimum speed	m/s	19
$v_{\max}$	maximum speed	m/s	25.5
n_v	DP speed discr. points	-	21
$T_{\min}$	minimum torque	Nm	-500
$T_{\max}$	maximum torque	Nm	2400
n_T	DP torque discr. points	-	37
$F_{\text{b,min}}$	minimum distance	kN	-20
$F_{\text{b,max}}$	maximum distance	kN	0
n_{F_b}	DP braking force discr. points	-	51
$g_{\min}$	minimum allowed gear	-	13
$g_{\max}$	maximum allowed gear	-	14
driving-alone control strategies			
$d_{\min}$	minimum distance	m	-100
$d_{\max}$	maximum distance	m	100
n_d	DP distance discr. points	-	157
vehicle-following control strategies			
$d_{\min}$	minimum distance	m	20
$d_{\max}$	maximum distance	m	100
n_d	DP distance discr. points	-	63

A. Simulation setup

The vehicle under control is characterized by the parameters' values displayed in Table I and is simulated using the model presented in Section III. The benchmark road is the highway stretch of 91 km displayed in Figure 6 between the cities of Södertalje and Jönåker, Sweden. The topography profile of such road is considered moderately hilly, with a slope grade varying between $\pm 3\,\%$. The values of the controller parameters are displayed in Table II.

The simulations run on a PC with a two-core CPU running at 2.4 GHz and 8 GB of memory RAM. The computation of the optimal closed-loop control law over the whole horizon H takes 1170 and 355 s for the driving-alone and the vehicle-following cases, respectively.

TABLE III

FUEL CONSUMPTION REDUCTION [%]

vehicle mass	driving-alone		vehicle-following		
	look-ahead w/o freewheel	look-ahead w/ freewheel	constant distance	look-ahead ACC w/o freewheel	look-ahead ACC w/ freewheel
30 t	0	4.1	12.4	14.5	18.6
40 t	0	3.1	8.9	12.5	15.5
50 t	0	2.7	5.1	10.3	12.7

B. Longitudinal control strategies comparison

In this section, we compare the performance of multiple longitudinal control strategies achieved with the proposed controller formulation. The mass of the vehicle under control varies in the different simulation sets between 30, 40 and 50 t. The preceding vehicle, when present, has a mass of 40 t for all the simulations. The control strategies that we compare are divided in the two following categories:

- driving-alone control strategies:
  - *look-ahead w/o freewheeling*: the vehicle under control optimizes its speed trajectory exploiting road topography information without using freewheeling. This is achieved by redefining $C_d(d) = C_{d,0}$ and $g_r \in \mathcal{G}$;
  - *look-ahead w/ freewheeling*: similarly to the previous case but allowing freewheeling, i.e., $g_r \in \{0\} \cup \mathcal{G}$;
- vehicle-following control strategies[3]:
  - *constant distance*: the vehicle under control keeps a fixed distance from the preceding one, equal to minimum allowed distance;
  - *look-ahead ACC w/o freewheeling*: the vehicle under control optimizes its speed trajectory exploiting topography information and the knowledge of the preceding vehicle speed trajectory without using freewheeling, i.e., $g_r \in \mathcal{G}$;
  - *look-ahead ACC w/ freewheeling*: similarly to the previous case but allowing freewheeling, i.e., $g_r \in \{0\} \cup \mathcal{G}$.

The fuel consumption reduction for all combinations of control strategies and vehicle masses is summarized in Table III. The saved fuel is normalized with respect to the fuel consumption of the *look-ahead w/o freewheeling* controller case.

Starting by the analysis of the driving-alone control strategies, we can notice that the exploitation of freewheeling allows to save between 2.7 and 4.1 % of fuel. In order to understand why, we can turn our attention to Figure 7 that shows a portion of the simulation results (between km 15 and 25) for the 40 t vehicle case. In the freewheeling case, the vehicle under control exhibits the so-called pulse & glide behavior. By alternating phases of freewheeling and traction

[3]The preceding vehicle has a mass of 40 t, uses the *look-ahead w/o freewheeling* control strategy and its trajectory is known to the vehicle under control.

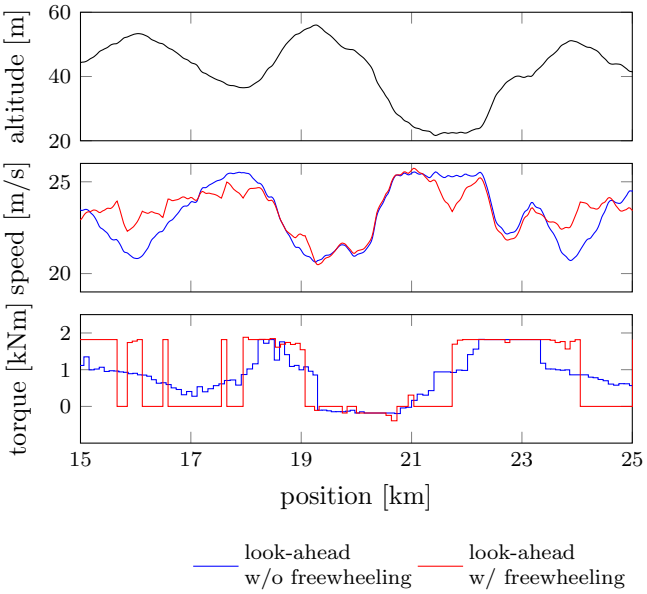

Fig. 7. Simulation results for a heavy-duty vehicle of 40 tons driving alone and using look-ahead control with and without freewheeling. The torque displayed in the last plot includes the engine torque and a scaled version of the braking force.

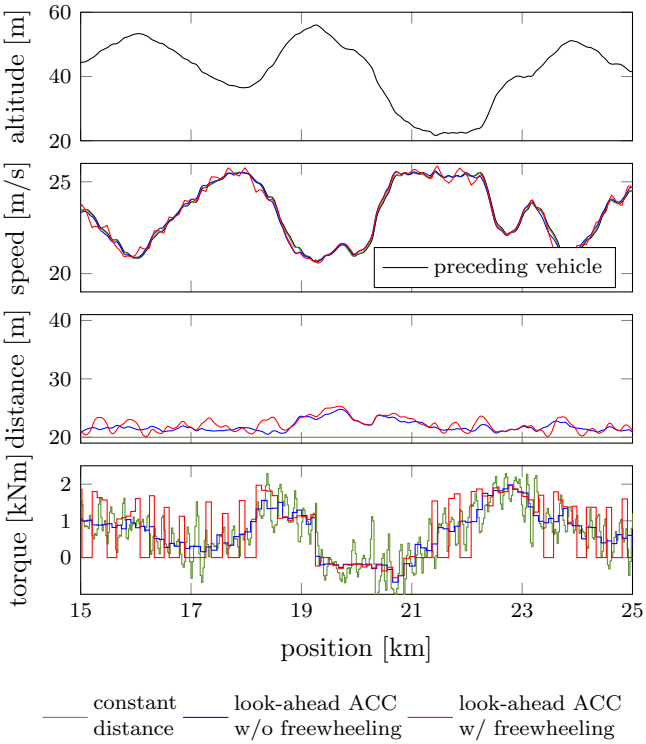

Fig. 8. Simulation results for a 40 t vehicle using multiple vehicle-following control strategies[3]. The torque plot is explained in the caption of Figure 7.

at the optimal torque (approximately 2 kNm, see Figure 5), the vehicle is able to use the engine in a more efficient way, resulting in the registered reduction in fuel consumption.

Let's now focus on the vehicle-following control strategies and, in particular, in the homogeneous platoon case (summarized in the second row of Table III), for which simulation results are displayed in Figure 8. Here, we recall that the preceding vehicle uses the *look-ahead w/o freewheeling* control. The registered fuel consumption reduction in all three cases is due to the reduced aerodynamic drag caused by the short inter-vehicular distance. The *constant distance* case represents the reference case, where the vehicle is controlled such that the distance is always equal to the minimum allowed. Although the aerodynamic drag reduction is maximized, as noticeable in the last plot of Figure 8, the vehicle under control often needs to brake. The braking is due to two reasons:

- first, the reduced aerodynamic drag translates in braking when the preceding vehicle is costing;
- second, since the preceding vehicle experiences the changes of slope grade before the vehicle under control, in order to keep a fixed distance, the vehicle under control needs to apply a larger longitudinal force when the slope grade is decreasing, and a smaller longitudinal force when the slope grade increases. The smaller longitudinal force phases can result in the braking of the vehicle under control when the preceding is exhibiting a close-to-coasting behavior. This behavior has been also experienced in the experiments presented in [20], where a constant headway gap has been used.

The optimization that takes place in the two *look-ahead ACC* cases, guarantees that the described braking phases are avoided. This results in a reduced fuel consumption with respect to the *constant distance* case, as summarized in Table III. Furthermore, the availability of freewheeling in the last case allows the vehicle to pulse & glide while keeping a short inter-vehicular distance, resulting in an additional fuel saving comparable to the fuel-saving achieved by pulsing & gliding in the driving-alone control case.

Finally, we analyze the vehicle-following control strategies for the heterogeneous platoon case (summarized in the first and third row of Table III). The *constant distance* controller performance deteriorates relatively to the *look-ahead ACC* cases with the increase of the controlled vehicle mass. This is due to the increase of the costing acceleration during downhills with the vehicle mass. This is noticeable in the simulation results for the 50 t vehicle case displayed in Figure 9, where the vehicle under control needs to brake more (and therefore wastes more energy) with respect to the 40 t vehicle case displayed in Figure 8. This problem is handled by the *look-ahead ACC* controllers by increasing the inter-vehicular distance before downhills, as evident in Figure 9.

To conclude, the use of look-ahead control strategies turns up to be more relevant in heavier follower vehicle cases.

VII. CONCLUSIONS AND FUTURE WORKS

In this paper, we studied the problem of how to fuel-optimally follow a vehicle whose future speed trajectory is

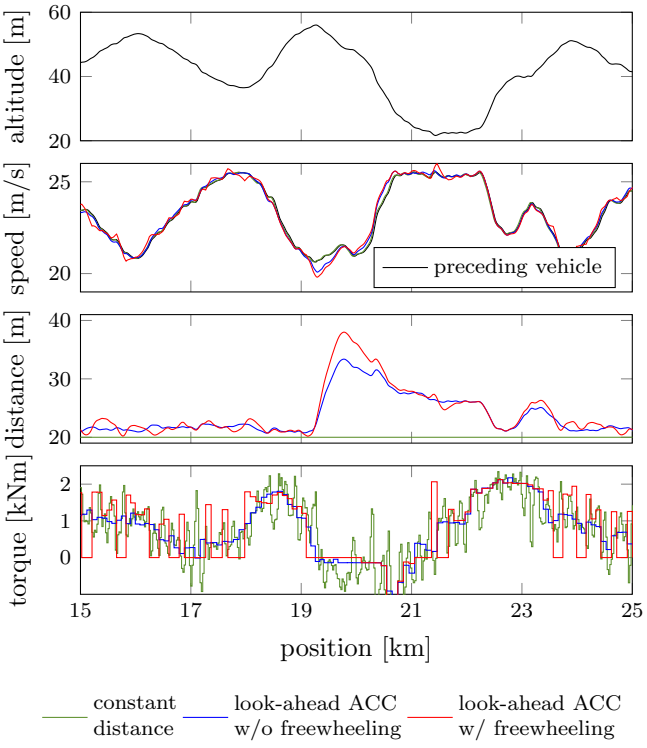

Fig. 9. Simulation results for a 50 t vehicle using multiple vehicle-following control strategies[3]. The torque plot is explained in the caption of Figure 7.

known. We proposed an optimal control problem formulation that describes the problem and we discussed how such problem can be solved by dynamic programming. By means of simulations, we showed how the proposed controller is able to combine the benefits of keeping a short inter-vehicular distance with those of freewheeling, achieving fuel saving up to 18 % with respect to the use of a look-ahead control.

The simulation study showed promising results in the scenario where the preceding vehicle future trajectory is fully known. We believe that continuing the efforts toward the design of a commercially deployable product will be extremely beneficial for both the freight transport sector and our environment. This requires to study how to handle uncertainties and updates in the preceding vehicle trajectory, and to focus on the real-time implementability problem.

A possible research direction consists in extending the presented work by applying a receding horizon approach to the proposed controller. In such framework, however, it is important to ensure that the updated trajectories of the preceding vehicle do not excessively deteriorate the performance of the vehicle under control (e.g., by leading it to brake). This could be achieved, for example, by controlling the preceding vehicle with a similar optimal control framework that exploits the knowledge of the follower vehicle state in its optimization.

Another research direction consists in investigating the applicability of reinforcement learning (also known as neuro-dynamic programming) methods on the presented problem. Simulation results have shown that the vehicle under control alternates between a finite number of optimal behaviors (i.e., optimal torque traction, freewheeling and braking). If we are able to learn for which regions in the state-parameter space each behavior is optimal, we could syntetize a fast online controller suitable for real-time implementation.

ACKNOWLEDGMENTS

We gratefully acknowledge the Swedish Governmental Agency for Innovation Systems (VINNOVA) through the FFI program, the Swedish Research Council and the Knut and Alice Wallenberg Foundation for their financial support.

REFERENCES

[1] European Commission. Energy Roadmap 2050. Technical report, Brussels, 2011.
[2] European Commission. White paper – Roadmap to a single European transport area: towards a competitive and resource efficient transport system. 2011.
[3] European Commission. *EU Transport in Figures 2016*. Publications Office of the European Union, Luxembourg, Luxembourg, 2016.
[4] U.S. Bureau of Transportation Statistics. *Pocket Guide to Transportation*. Washington, DC, USA, 2016.
[5] OECD/ITF. *ITF Transport Outlook 2017*. OECD Publishing, Paris, France, 2017.
[6] Scania AB. Annual report 2013. Technical report, Scania AB, aug 2013.
[7] S.E. Shladover. Recent international activity in cooperative vehicle-highway automation systems. Technical report, California PATH Program, 2012.
[8] J. Carbaugh, D. N. Godbole, and R. Sengupta. Safety and capacity analysis of automated and manual highway systems. *Transportation Research Part C: Emerging Technologies*, 6(1-2):69–99, 1998.
[9] L. Alvarez and R. Horowitz. Safe platooning in automated highway systems. Technical report, California PATH Program, 1997.
[10] T. Robinson and E. Coelingh. Operating platoons on public motorways: an introduction to the SARTRE platooning programme. In *17th world congress on intelligent transport systems*, Busan , South Korea, 2010.
[11] P. Kavathekar and Y. Chen. Vehicle platooning: A brief survey and categorization. *ASME 2011 International Design Engineering Technical Conferences and Computers and Information in Engineering Conference*, (November 2014):829–845, 2011.
[12] D. Swaroop and J. K. Hedrick. String stability of interconnected systems. *IEEE Transactions on Automatic Control*, 41(3):349–357, mar 1996.
[13] J. I. Ge and G. Orosz. Dynamics of connected vehicle systems with delayed acceleration feedback. *Transportation Research Part C: Emerging Technologies*, 46:46–64, 2014.
[14] S. Biswas, R. Tatchikou, and F. Dion. Vehicle-to-vehicle wireless communication protocols for enhancing highway traffic safety. *IEEE Communications Magazine*, 44(1):74–82, 2006.
[15] S. Tsugawa, S. Jeschke, and S. E. Shladover. A Review of Truck Platooning Projects for Energy Savings. *IEEE Transactions on Intelligent Vehicles*, 8858(c):1–1, 2016.
[16] A. Alam, A. Gattami, and K. H. Johansson. An experimental study on the fuel reduction potential of heavy duty vehicle platooning. In *13th International IEEE Conference on Intelligent Transportation Systems*, pages 306–311, Madeira Island, Portugal, sep 2010.
[17] N. Murgovski, B. Egardt, and M. Nilsson. Cooperative energy management of automated vehicles. *Control Engineering Practice*, 57(December):84–98, 2016.
[18] V. Turri, B. Besselink, and K. H. Johansson. Cooperative look-ahead control for fuel-efficient and safe heavy-duty vehicle platooning. *IEEE Transactions on Control Systems Technology*, 25(1):12–28, 2017.
[19] R. Bellman. *Dynamic Programming*. Princeton University Press, Princeton, NJ, USA, 1957.
[20] A. Alam, B. Besselink, V. Turri, J. Mårtensson, and K. H. Johansson. Heavy-duty vehicle platooning towards sustainable freight transportation. *IEEE Control Systems Magazine*, 35(6):34–56, 2015.